Asymmetric polychromatic tripartite entanglement from interlinked $\chi^{(2)}$ parametric interactions

M. K. Olsen and A. S. Bradley

ARC Centre of Excellence for Quantum-Atom Optics, School of Physical Sciences, University of Queensland, Brisbane, Queensland 4072, Australia

We examine the tripartite entanglement properties of an optical system using interlinked $\chi^{(2)}$ interactions, recently studied experimentally in terms of its phase-matching properties by Bondani *et al.* [Opt. Express **14**, 21, 9838 (2006)]. We show that the system produces output modes at three distinct frequencies which are genuinely tripartite entangled, and analyze this entanglement in terms of different measurable correlations. We show that, due to the asymmetry of the process, the detection of this entanglement depends crucially on the correlation functions that are measured. We find that some of the correlations found in the literature fail to register the entanglement, in contrast to symmetric systems, for which the actual choice of correlation to be measured makes little difference.

I. INTRODUCTION

Entanglement is a property that is central to quantum mechanics and helps to distinguish it from classical mechanics. A vast amount of work has been undertaken on discrete-variable entanglement, with somewhat less having been performed on the continuous-variable case. It is the latter which interests us in this work, particularly as regards the entanglement of three asymmetric optical modes with different frequencies. We will focus on an experimentally realized system which links two $\chi^{(2)}$ interactions in a combined down-conversion and sum frequency generation process [1], and examine its utility for the production of states that exhibit full tripartite entanglement. As far as we are aware, full tripartite entanglement has been unambiguously demonstrated only by mixing squeezed vacua with linear optical elements [2,3], although other methods that create the entanglement using an actual nonlinear interaction are under investigation, using both cascaded and concurrent $\chi^{(2)}$ processes [4–7]. Two of the features that distinguish the scheme realized by Bondani and co-workers are the fact that it entangles three fields at different wavelengths, which we shall call polychromatic entanglement, and also that it is totally asymmetric, with none of the three modes being interchangeable. In the sense of entangling fields at different frequencies, this scheme is an extension from two to three modes of the harmonic (bichromatic) entanglement previously analyzed for a nonlinear intracavity system by Grosse *et al.* [8].

The definition of tripartite entanglement for three-mode systems is a little more subtle than that for bipartite entanglement, with different classes of entanglement having been defined, depending on how the system density matrix may be partitioned [9]. The classifications range from fully inseparable, which means that the density matrix is not separable for any grouping of the modes, to fully separable, where the three modes are not entangled in any way. For the fully inseparable case, van Loock and Furusawa [10], who call this genuine tripartite entanglement, have derived inequalities that are easily applicable to continuous-variable processes. More recently, Bradley *et al.* [6] have defined three-mode Einstein-Podolsky-Rosen (EPR) [12] type criteria, and Olsen

et al. [11] have given a rigorous proof that these also provide sufficient, but not necessary, conditions for the demonstration of genuine tripartite entanglement. In this paper we will begin by reviewing the definitions of these entanglement criteria and then apply them to the outputs of the Bondani scheme to quantify entanglement correlations which may in principle be measured experimentally. There are also different possible classifications of the entangled systems in terms of their symmetry properties, with fully symmetric systems remaining equivalent under any interchange of the mode indices, bisymmetric systems allowing for two of the three indices to be interchanged, and asymmetric systems for which none of the indices may be interchanged. As examples, the schemes of Refs. [3,6] are fully symmetric while the scheme we analyze here is asymmetric. As we will demonstrate, this asymmetry means that a careful choice must be made of the criteria to be measured, with some choices completely failing to detect the genuine tripartite entanglement that this scheme exhibits.

II. CRITERIA FOR TRIPARTITE ENTANGLEMENT

We begin by giving the optical quadrature definitions we will use in our analysis, as the exact form of the inequalities will depend on these. For three modes described by the bosonic annihilation operators $\hat{a}_j$, where $j=1,2,3$, we define quadrature operators for each mode as

$$\hat{X}_j = \hat{a}_j + \hat{a}_j^\dagger, \quad \hat{Y}_j = -i(\hat{a}_j - \hat{a}_j^\dagger), \tag{1}$$

so that the Heisenberg uncertainty principle requires $V(\hat{X}_j)V(\hat{Y}_j) \geq 1$.

A. Three-mode Einstein-Podolsky-Rosen correlations

The EPR argument was introduced in 1935 in an attempt to show that quantum mechanics could not be both complete and consistent with local realism [12]. Schrödinger replied that same year by introducing the concept of entangled states which were not compatible with classical notions such as local realism [13]. In 1989 Reid [14], and Reid and

Drummond [15] proposed a physical test of the EPR paradox using optical quadrature amplitudes, which are mathematically identical to the position and momentum originally considered by EPR. Reid later expanded on this work, demonstrating that the satisfaction of the 1989 two-mode EPR criterion always implies bipartite quantum entanglement [16]. Tan made a similar demonstration in the context of teleportation, considering the outputs from a nondegenerate optical parameteric amplifier mixed on a beam splitter [17]. In this paper we use an extension of Reid's original approach to the case of tripartite correlations, where quadratures of three different optical modes are involved. This extension was developed and formally proven to demonstrate the presence of tripartite entanglement by Olsen *et al.* in Ref. [11]; so that for notational simplicity, we shall call these the Olsen-Bradley-Reid (OBR) criteria.

There are two ways to consider the experimentally accessible form of the OBR criteria, depending on whether we use information from two quadratures to infer properties of the other, or information from one to infer combined properties of the other two. In the first case, we make a linear estimate of the quadrature $\hat{X}_i$ from the properties of the combined mode $j+k$, using parameters which can be optimized, both experimentally and theoretically [14,18]. It has been shown [11,15] that minimizing the root-mean-square error in this estimate leads to an optimal inferred variance,

$$V^{inf}(\hat{X}_i) = V(\hat{X}_i) - \frac{[V(\hat{X}_i, \hat{X}_j \pm \hat{X}_k)]^2}{V(\hat{X}_j \pm \hat{X}_k)}, \qquad (2)$$

where $V(\hat{A}, \hat{B}) = \langle \hat{A}\hat{B} \rangle - \langle \hat{A} \rangle \langle \hat{B} \rangle$. We follow the same procedure for the $\hat{Y}$ quadratures to give expressions which may be obtained by swapping each $\hat{X}$ for a $\hat{Y}$ in the above to give

$$V^{inf}(\hat{Y}_i) = V(\hat{Y}_i) - \frac{[V(\hat{Y}_i, \hat{Y}_j \pm \hat{Y}_k)]^2}{V(\hat{Y}_j \pm \hat{Y}_k)}. \qquad (3)$$

A demonstration of the EPR paradox can be claimed whenever

$$V^{inf}(\hat{X}_i) V^{inf}(\hat{Y}_i) < 1. \qquad (4)$$

As was proven [11], this demonstration—for the three possible values of *i*—is then sufficient to establish tripartite entanglement, without any assumptions made about whether or not the states involved are Gaussian.

Following the same logic, if we use the properties of mode *i* to infer properties of the combined mode $j+k$, we find that there is a demonstration of the other three-mode form of the EPR paradox whenever

$$V^{inf}(\hat{X}_j \pm \hat{X}_k) V^{inf}(\hat{Y}_j \pm \hat{Y}_k) < 4, \qquad (5)$$

where, for example,

$$V^{inf}(\hat{X}_j \pm \hat{X}_k) = V(\hat{X}_j \pm \hat{X}_k) - \frac{[V(\hat{X}_i, \hat{X}_j \pm \hat{X}_k)]^2}{V(\hat{X}_i)}. \qquad (6)$$

As indicated above, this demonstration for the three possible combinations also serves to establish complete inseparability of the density matrix.

B. The van Loock–Furusawa inequalities

A set of conditions that are also sufficient to demonstrate tripartite entanglement for any quantum state have been derived by van Loock and Furusawa [10]. Using our quadrature definitions, the van Loock–Furusawa (VLF) conditions give a set of inequalities, which we shall refer to as the VLF inequalities,

$$V_{12} = V(\hat{X}_1 - \hat{X}_2) + V(\hat{Y}_1 + \hat{Y}_2 + g_3\hat{Y}_3) \geq 4,$$

$$V_{13} = V(\hat{X}_1 - \hat{X}_3) + V(\hat{Y}_1 + g_2\hat{Y}_2 + \hat{Y}_3) \geq 4,$$

$$V_{23} = V(\hat{X}_2 - \hat{X}_3) + V(g_1\hat{Y}_1 + \hat{Y}_2 + \hat{Y}_3) \geq 4, \qquad (7)$$

where $V(A) \equiv \langle A^2 \rangle - \langle A \rangle^2$ and the g_i are arbitrary real numbers. As shown in Ref. [10], the violation of the first inequality still leaves the possibility that mode 3 could be separated from modes 1 and 2, but this possibility is negated by violation of the second. Therefore, if any two of these inequalities are violated, the system is fully inseparable and genuine tripartite entanglement is guaranteed. We note also that genuine tripartite entanglement may still be possible without the violation of any of these inequalities.

We will now investigate optimization of the VLF criteria, using the freedom allowed in the choice of the g_i, which are arbitrary real parameters. A simple minimization of the right-hand sides of Eq. (7) with respect to the g_i gives

$$g_1 = \frac{-(\langle \hat{Y}_1\hat{Y}_2 \rangle + \langle \hat{Y}_1\hat{Y}_3 \rangle)}{\langle \hat{Y}_1^2 \rangle},$$

$$g_2 = \frac{-(\langle \hat{Y}_1\hat{Y}_2 \rangle + \langle \hat{Y}_2\hat{Y}_3 \rangle)}{\langle \hat{Y}_2^2 \rangle},$$

$$g_3 = \frac{-(\langle \hat{Y}_1\hat{Y}_3 \rangle + \langle \hat{Y}_2\hat{Y}_3 \rangle)}{\langle \hat{Y}_3^2 \rangle}. \qquad (8)$$

The required variances can now be written as, for example,

$$V(\hat{X}_1 - \hat{X}_2) = \langle \hat{X}_1^2 \rangle + \langle \hat{X}_2^2 \rangle - 2\langle \hat{X}_1\hat{X}_2 \rangle,$$

$$V(\hat{Y}_1 + \hat{Y}_2 + g_3\hat{Y}_3) = \langle \hat{Y}_1^2 \rangle + \langle \hat{Y}_2^2 \rangle + g_3^2\langle \hat{Y}_3^2 \rangle + 2[\langle \hat{Y}_1\hat{Y}_2 \rangle$$
$$+ g_3(\langle \hat{Y}_1\hat{Y}_3 \rangle + \langle \hat{Y}_2\hat{Y}_3 \rangle)]. \qquad (9)$$

Once this optimization process has taken place, we find that, for example,

$$V(\hat{Y}_1 + \hat{Y}_2 + g_3\hat{Y}_3) = V(\hat{Y}_1 + \hat{Y}_2) - \frac{[V(\hat{Y}_3, \hat{Y}_1 + \hat{Y}_2)]^2}{V(\hat{Y}_3)},$$
(10)

where we recognize the right-hand side as an inferred variance as introduced in Ref. [11] to demonstrate the EPR paradox for three modes, and referred to above. The optimized correlations can now be written as

$$V_{12} = V(\hat{X}_1 - \hat{X}_2) + V^{inf}(\hat{Y}_1 + \hat{Y}_2) \geq 4,$$

$$V_{13} = V(\hat{X}_1 - \hat{X}_3) + V^{inf}(\hat{Y}_1 + \hat{Y}_3) \geq 4,$$

$$V_{23} = V(\hat{X}_2 - \hat{X}_3) + V^{inf}(\hat{Y}_2 + \hat{Y}_3) \geq 4.$$
(11)

We see that the VLF criteria now have the same form as the Duan and Simon criteria for bipartite entanglement [19,20], but with the actual variance $V(\hat{Y}_j + \hat{Y}_k)$ replaced by the inferred variance $V^{inf}(\hat{Y}_j + \hat{Y}_k)$ of Eq. (5). We note that the violation of two out of three of the inequalities is sufficient to demonstrate full inseparability.

It is also possible to develop a single sufficient condition to detect genuine tripartite entanglement from the combined quadrature variances [10,21]. In this case we find that, for a fully inseparable three-mode system, it is sufficient to measure

$$V_{ijk} = V(\hat{X}_i - (\hat{X}_j + \hat{X}_k)/\sqrt{2}) + V(\hat{Y}_i + (\hat{Y}_j + \hat{Y}_k)/\sqrt{2}) < 4,$$
(12)

where the mode indices i,j,k are all different, to demonstrate this inseparability. For a symmetric scheme, the values of the indices would not be important, with any choice giving an equal result. However, as we show below, this is not the case when the system is asymmetric.

III. SYSTEM AND EQUATIONS OF MOTION

The interaction Hamiltonian used by Bondani *et al.* [1] uses an undepleted pump approximation and we will begin with a more complete form that quantizes all the interacting fields. The Hamiltonian describes the coupling of five modes of the electromagnetic field in a phase-matched simultaneous sum frequency generation and down-conversion process in a manner analogous to the schemes considered by Olsen and Bradley [7], and has previously been investigated by Ferraro *et al.* [5] and Smithers and Lu [22]. The full five-mode Hamiltonian may be written as

$$\mathcal{H}_{int} = i\hbar(\chi_1\hat{a}_4\hat{a}_1^\dagger\hat{a}_3^\dagger + \chi_2\hat{a}_5\hat{a}_2^\dagger\hat{a}_3) + \text{H.c.},$$
(13)

where we have set the coupling coefficients as real. Due to energy conservation, $\omega_4 = \omega_1 + \omega_3$ and $\omega_2 = \omega_3 + \omega_5$, and the necessary phase-matching conditions are covered in Ref. [1]. In the experiment performed by Bondani *et al.*, the three fields produced in the interaction have wavelengths $\lambda_1 = 632.8$ nm, $\lambda_2 = 446.4$ nm, and $\lambda_3 = 778.2$ nm, so that any entanglement produced is between modes with markedly

different frequencies. This Hamiltonian approximately describes a down-conversion process cascaded with a sum frequency generation process where one of the down-converted modes becomes an auxiliary pump mode for the frequency generation process. It gives a simplified description because it does not include effects such as dispersion within the nonlinear medium, for example. A more accurate method of analyzing these types of processes has been given by Raymer *et al.* [23], but the approximations we are using do serve to set upper limits on the squeezing and entanglement available from a more realistic treatment of the physical process [24].

However, given the above caveat, it is instructive to examine the analytical solutions that may be obtained using an undepleted pump approximation as without a cavity the interaction strengths tend to be small and this approximation is generally accurate. Setting $\kappa_1 = \chi_1\langle\hat{a}_4(0)\rangle$ and $\kappa_2 = \chi_2\langle\hat{a}_5(0)\rangle$ as real positive constants, the Hamiltonian may be written

$$\mathcal{H}_{int} = i\hbar[\kappa_1(\hat{a}_1^\dagger\hat{a}_3^\dagger - \hat{a}_1\hat{a}_3) + \kappa_2(\hat{a}_2^\dagger\hat{a}_3 - \hat{a}_2\hat{a}_3^\dagger)],$$
(14)

from which we find the Heisenberg equations of motion,

$$\frac{d\hat{a}_1}{dt} = \kappa_1\hat{a}_3^\dagger,$$

$$\frac{d\hat{a}_2}{dt} = \kappa_2\hat{a}_3,$$

$$\frac{d\hat{a}_3}{dt} = \kappa_1\hat{a}_1^\dagger - \kappa_2\hat{a}_2.$$
(15)

For later convenience we will rewrite the above as equations of motion for the quadrature operators, finding

$$\frac{d\hat{X}_1}{dt} = \kappa_1\hat{X}_3,$$

$$\frac{d\hat{Y}_1}{dt} = -\kappa_1\hat{Y}_3,$$

$$\frac{d\hat{X}_2}{dt} = \kappa_2\hat{X}_3,$$

$$\frac{d\hat{Y}_2}{dt} = \kappa_2\hat{Y}_3,$$

$$\frac{d\hat{X}_3}{dt} = \kappa_1\hat{X}_1 - \kappa_2\hat{X}_2,$$

$$\frac{d\hat{Y}_3}{dt} = -\kappa_1\hat{Y}_1 - \kappa_2\hat{Y}_2.$$
(16)

These equations can now be solved analytically to give the solutions for the operators as functions of their initial values, which will all be zero for this system. However, due to bosonic commutation relations, not all the moments vanish

and at $t=0$ with all the output fields as vacuum, we have $\langle \hat{X}_i(0)\hat{X}_j(0)\rangle = \langle \hat{Y}_i(0)Y_j(0)\rangle = \delta_{ij}$. This is all the information we need to find useful time-dependent solutions for the variances and covariances needed for the correlations which establish tripartite entanglement.

A. Hyperbolic solutions

We find that there are three classes of solutions for different regimes, depending on whether $\kappa_2^2 > \kappa_1^2$, $\kappa_2^2 < \kappa_1^2$ or $\kappa_1^2 = \kappa_2^2$. The last of these was treated in Ref. [7] and we will not consider it further here. For $\kappa_2^2 > \kappa_1^2$, Ω is imaginary and the solutions are periodic, while for $\kappa_2^2 < \kappa_1^2$ the solutions are hyperbolic. We will begin with the correlations for the hyperbolic solutions, as this is the operating regime of the Bondani *et al.* experiment [1].

Setting $\Omega = \sqrt{\kappa_1^2 - \kappa_2^2}$, we find these solutions as

$$\hat{X}_1(t) = \frac{\kappa_1^2 \cosh \Omega t - \kappa_2^2}{\Omega^2}\hat{X}_1(0) - \frac{\kappa_1\kappa_2(\cosh \Omega t - 1)}{\Omega^2}\hat{X}_2(0)$$
$$+ \frac{\kappa_1 \sinh \Omega t}{\Omega}\hat{X}_3(0),$$

$$\hat{Y}_1(t) = \frac{\kappa_1^2 \cosh \Omega t - \kappa_2^2}{\Omega^2}\hat{Y}_1(0) + \frac{\kappa_1\kappa_2(\cosh \Omega t - 1)}{\Omega^2}\hat{Y}_2(0)$$
$$- \frac{\kappa_1 \sinh \Omega t}{\Omega}\hat{Y}_3(0),$$

$$\hat{X}_2(t) = \frac{\kappa_1\kappa_2(\cosh \Omega t - 1)}{\Omega^2}\hat{X}_1(0) + \frac{\kappa_1^2 - \kappa_2^2 \cosh \Omega t}{\Omega^2}\hat{X}_2(0)$$
$$+ \frac{\kappa_2 \sinh \Omega t}{\Omega}\hat{X}_3(0),$$

$$\hat{Y}_2(t) = -\frac{\kappa_1\kappa_2(\cosh \Omega t - 1)}{\Omega^2}\hat{Y}_1(0) + \frac{\kappa_1^2 - \kappa_2^2 \cosh \Omega t}{\Omega^2}\hat{Y}_2(0)$$
$$+ \frac{\kappa_2 \sinh \Omega t}{\Omega}\hat{Y}_3(0),$$

$$\hat{X}_3(t) = \frac{\kappa_1 \sinh \Omega t}{\Omega}\hat{X}_1(0) - \frac{\kappa_2 \sinh \Omega t}{\Omega}\hat{X}_2(0) + \hat{X}_3(0)\cosh \Omega t,$$

$$\hat{Y}_3(t) = -\frac{\kappa_1 \sinh \Omega t}{\Omega}\hat{Y}_1(0) - \frac{\kappa_2 \sinh \Omega t}{\Omega}\hat{Y}_2(0) + \hat{Y}_3(0)\cosh \Omega t,$$

$$(17)$$

which contain all the information needed to calculate the VLF and OBR correlations in the approximations we are using, except in the case where $\kappa_1^2 = \kappa_2^2$. In this case the above solutions are not well defined but the equations may still be solved using stochastic integration, as was done in Ref. [7]. For $\kappa_1^2 > \kappa_2^2$, the time-dependent moments that we need are

$$\langle \hat{X}_1^2\rangle = \langle \hat{Y}_1^2\rangle = 1 + \frac{2\kappa_1^2}{\Omega^4}[\kappa_1^2 \sinh^2 \Omega t + 2\kappa_2^2(1 - \cosh \Omega t)],$$

$$\langle \hat{X}_2^2\rangle = \langle \hat{Y}_2^2\rangle = 1 + \frac{1}{\Omega^4}[2\kappa_1^2\kappa_2^2(\cosh \Omega t - 1)^2],$$

$$\langle \hat{X}_3^2\rangle = \langle \hat{Y}_3^2\rangle = 1 + \frac{2\kappa_1^2 \sinh^2 \Omega t}{\Omega^2},$$

$$\langle \hat{X}_1\hat{X}_2\rangle = -\langle \hat{Y}_1\hat{Y}_2\rangle = \frac{\kappa_1\kappa_2}{\Omega^4}[(\kappa_1^2 + \kappa_2^2)(\cosh \Omega t - 1)^2$$
$$+ \Omega^2 \sinh^2 \Omega t],$$

$$\langle \hat{X}_1\hat{X}_3\rangle = -\langle \hat{Y}_1\hat{Y}_3\rangle = \frac{2\kappa_1 \sinh \Omega t}{\Omega^3}(\kappa_1^2 \cosh \Omega t - \kappa_2^2),$$

$$\langle \hat{X}_2\hat{X}_3\rangle = \langle \hat{Y}_2\hat{Y}_3\rangle = \frac{2\kappa_1^2\kappa_2}{\Omega^3}(\cosh \Omega t - 1)\sinh \Omega t. \quad (18)$$

We note here that the above expectation values are actually the variances and covariances for the quadratures, as the expectation values of the amplitudes are all zero.

B. Periodic solutions

We will now look at the case where $\kappa_2^2 > \kappa_1^2$, which leads to solutions expressed in terms of periodic functions. Setting $\xi = \sqrt{\kappa_2^2 - \kappa_1^2}$, we find

$$\hat{X}_1(t) = \frac{\kappa_2^2 - \kappa_1^2 \cos \xi t}{\xi^2}\hat{X}_1(0) + \frac{\kappa_1\kappa_2(\cos \xi t - 1)}{\xi^2}\hat{X}_2(0)$$
$$+ \frac{\kappa_1 \sin \xi t}{\xi}\hat{X}_3(0),$$

$$\hat{Y}_1(t) = \frac{\kappa_2^2 - \kappa_1^2 \cos \xi t}{\xi^2}\hat{Y}_1(0) - \frac{\kappa_1\kappa_2(\cos \xi t - 1)}{\xi^2}\hat{Y}_2(0)$$
$$+ \frac{\kappa_1 \sin \xi t}{\xi}\hat{Y}_3(0),$$

$$\hat{X}_2(t) = \frac{\kappa_1\kappa_2(1 - \cos \xi t)}{\xi^2}\hat{X}_1(0) + \frac{\kappa_2^2 \cos \xi t - \kappa_1^2}{\xi^2}\hat{X}_2(0)$$
$$+ \frac{\kappa_2 \sin \xi t}{\xi}\hat{X}_3(0),$$

$$\hat{Y}_2(t) = \frac{\kappa_1\kappa_2(\cos \xi t - 1)}{\xi^2}\hat{Y}_1(0) + \frac{\kappa_2^2 \cos \xi t - \kappa_1^2}{\xi^2}\hat{Y}_2(0)$$
$$+ \frac{\kappa_2 \sin \xi t}{\xi}\hat{Y}_3(0),$$

$$\hat{X}_3(t) = \frac{\kappa_1 \sin \xi t}{\xi}\hat{X}_1(0) - \frac{\kappa_2 \sin \xi t}{\xi}\hat{X}_2(0) + \hat{X}_3(0)\cos \xi t,$$

$$\hat{Y}_3(t) = -\frac{\kappa_1 \sin \xi t}{\xi}\hat{Y}_1(0) - \frac{\kappa_2 \sin \xi t}{\xi}\hat{Y}_2(0) + \hat{Y}_3(0)\cos \xi t,$$
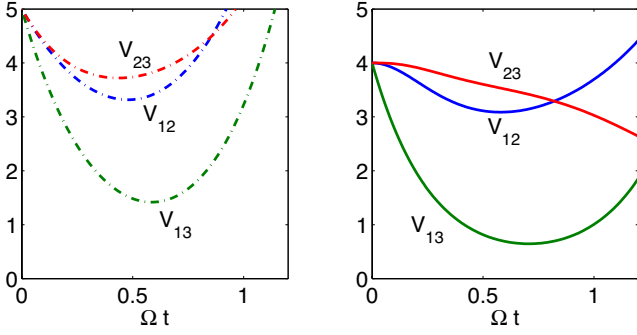
$$(19)$$

which lead to the solutions for the moments,

FIG. 1. (Color online) The analytical solutions of the VLF correlations, with $\kappa_1 = 1.2\kappa_2$. Any two of the correlations falling below 4 is sufficient to demonstrate that genuine tripartite entanglement is present. The solid lines use the optimized expressions. All quantities shown in these and subsequent graphs are dimensionless.

$$\langle \hat{X}_1^2 \rangle = \langle \hat{Y}_1^2 \rangle = 1 + \frac{2\kappa_1^2[2\kappa_2^2(1 - \cos \xi t) - \kappa_1^2 \sin^2 \xi t]}{\xi^4},$$

$$\langle \hat{X}_2^2 \rangle = \langle \hat{Y}_2^2 \rangle = 1 + \frac{2\kappa_1^2 \kappa_2^2 (\cos \xi t - 1)^2}{\xi^4},$$

$$\langle \hat{X}_3^2 \rangle = \langle \hat{Y}_3^2 \rangle = 1 + \frac{2\kappa_1^2 \sin^2 \xi t}{\xi^2},$$

$$\langle \hat{X}_1 \hat{X}_2 \rangle = -\langle \hat{Y}_1 \hat{Y}_2 \rangle = \frac{2\kappa_1 \kappa_2}{\xi^4}[(\kappa_1^2 + \kappa_2^2)(1 - \cos \xi t) - \kappa_1^2 \sin^2 \xi t],$$

$$\langle \hat{X}_1 \hat{X}_3 \rangle = -\langle \hat{Y}_1 \hat{Y}_3 \rangle = \frac{\kappa_1}{\xi^3}[2\kappa_2^2 \sin \xi t - \kappa_1^2 \sin 2\xi t],$$

$$\langle \hat{X}_2 \hat{X}_3 \rangle = \langle \hat{Y}_2 \hat{Y}_3 \rangle = \frac{2\kappa_1^2 \kappa_2 \sin \xi t}{\xi^3}[1 - \cos \xi t]. \quad (20)$$

IV. ENTANGLEMENT RESULTS

Analytical expressions can be found for both the VLF and OBR correlations using the results of Eqs. (18) and (20), but as these can be rather unwieldy we will present our results graphically. In the interests of compact notation we will use the shorthand V_{ij} for the correlation which contains $V(\hat{X}_i - \hat{X}_j)$. In Fig. 1 we show the results of the VLF correlations for the hyperbolic solutions, with $\kappa_1 = 1.2\kappa_2$. The dash-dotted lines are the basic expressions, without any optimization, and demonstrate that genuine tripartite entanglement is present over a small range of interaction strength. The solid lines are the expressions optimized as in Eq. (11) and are seen to violate the inequalities over a wider range. Perhaps the most useful effect of this optimization is that it allows for the demonstration of entanglement as soon as the interaction is nonzero, whereas the expressions without optimization need some finite interaction before any of them go below 4. This is not a contradiction as entanglement may be present
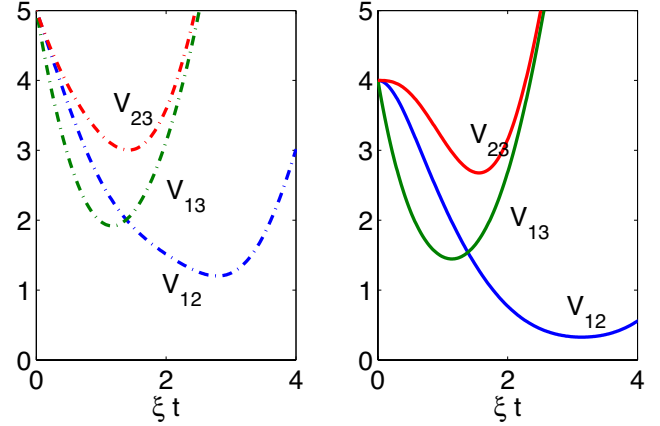

FIG. 2. (Color online) The analytical solutions of the VLF correlations, with $\kappa_2 = 1.8\kappa_1$. Any two of the correlations falling below 4 is sufficient to demonstrate that genuine tripartite entanglement is present. The solid lines use the optimized expressions.

even if the inequalities are not violated, in contrast to the Duan and Simon criteria for Gaussian bipartite systems, which provide necessary and sufficient conditions [19,20]. We are not aware of any criteria for tripartite continuous-variable entanglement that provide both necessary and sufficient conditions using only second-order moments. In Fig. 2 we present results for the same correlations in the regime of periodic solutions, with $\kappa_2 = 1.8\kappa_1$. We again see that, as expected, the optimization procedure allows for demonstration of entanglement over a wider range of interaction strengths.

When we investigate the single correlations, V_{ijk} of Eq. (12), which are sufficient to demonstrate genuine tripartite entanglement, we find that the correct choice of the indices is crucial. As shown in Fig. 3, the only one of these correlations that detects the entanglement is V_{123}. In a symmetric system the choice of indices would be of no importance, with all three possibilities giving the same result. However, this is perhaps not as much of a drawback as it may at first seem. If we consider the operator moments that are necessary to measure V_{123}, for example, we find that these are the six variances, $\langle \hat{X}_i^2 \rangle$ and $\langle \hat{Y}_i^2 \rangle$, and the covariances $\langle \hat{X}_1 \hat{X}_2 \rangle$, $\langle \hat{X}_1 \hat{X}_3 \rangle$, and $\langle \hat{X}_2 \hat{X}_3 \rangle$ (similarly for $\hat{Y}$). As these moments are all that are required to measure all three of the V_{ijk}, these can all be constructed from the same data set and the optimal correlation chosen. In fact, measurement of the 12 possible second-order moments allows for the measurement of any of the correlations we consider in this paper.

The three-mode EPR correlations

$$C_i^{OBR} = V^{inf}(\hat{X}_i)V^{inf}(\hat{Y}_i),$$

$$C_{jk}^{OBR} = V^{inf}(\hat{X}_j + \hat{X}_k)V^{inf}(\hat{Y}_j + \hat{Y}_k) \quad (21)$$

may be expressed in terms of the operator moment expectation values using

$$V^{inf}(\hat{X}_i) = \langle \hat{X}_i^2 \rangle - \frac{[\langle \hat{X}_i \hat{X}_j \rangle + \langle \hat{X}_i \hat{X}_k \rangle]^2}{\langle \hat{X}_j^2 \rangle + \langle \hat{X}_k^2 \rangle + 2\langle \hat{X}_j \hat{X}_k \rangle},$$
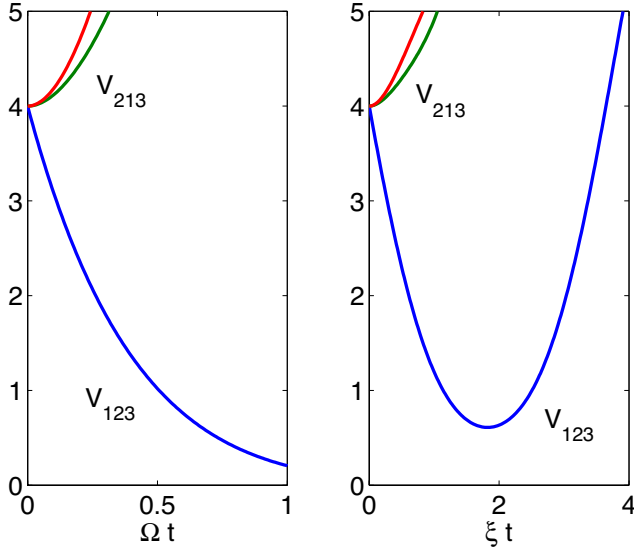
FIG. 3. (Color online) The analytical solutions for the V_{ijk} correlations of Eq. (12). On the left-hand side, $\kappa_1 = 1.2\kappa_2$, while on the right-hand side $\kappa_2 = 1.8\kappa_1$. Although any one of these being below 4 is sufficient to demonstrate genuine tripartite entanglement, we see that only a measurement of V_{123} detects the entanglement, with the other two (V_{312} is the upper line) always remaining above 4.

$$V^{inf}(\hat{Y}_i) = \langle \hat{Y}_i^2 \rangle - \frac{[\langle \hat{Y}_i \hat{Y}_j \rangle + \langle \hat{Y}_i \hat{Y}_k \rangle]^2}{\langle \hat{Y}_j^2 \rangle + \langle \hat{Y}_k^2 \rangle + 2\langle \hat{Y}_j \hat{Y}_k \rangle},$$

$$V^{inf}(\hat{X}_j + \hat{X}_k) = \langle \hat{X}_j^2 \rangle + \langle \hat{X}_k^2 \rangle + 2\langle \hat{X}_j \hat{X}_k \rangle - \frac{[\langle \hat{X}_i \hat{X}_j \rangle + \langle \hat{X}_i \hat{X}_k \rangle]^2}{\langle \hat{X}_i^2 \rangle},$$

$$V^{inf}(\hat{Y}_j + \hat{Y}_k) = \langle \hat{Y}_j^2 \rangle + \langle \hat{Y}_k^2 \rangle + 2\langle \hat{Y}_j \hat{Y}_k \rangle - \frac{[\langle \hat{Y}_i \hat{Y}_j \rangle + \langle \hat{Y}_i \hat{Y}_k \rangle]^2}{\langle \hat{Y}_i^2 \rangle}.$$

$$(22)$$

In Fig. 4 we give the results for C_i^{OBR} in both the periodic and hyperbolic regimes. Neither of these results, which come from inferring the properties of a single quadrature from the properties of a combined two-mode quadrature, gives evidence of genuine tripartite entanglement. In fact, all that these particular correlations succeed in demonstrating is that the combined density matrix ρ_{123} cannot be separated in the manner $\rho_{123} = \rho_1 \rho_{23}$, while leaving open the possibilities $\rho_{123} = \rho_2 \rho_{13}$ and $\rho_{123} = \rho_3 \rho_{12}$. This shows that choosing to measure these particular criteria to demonstrate entanglement would not be sensible, in contrast to the triply nonlinear system considered in Bradley *et al.* [6] and Olsen *et al.* [11], where the symmetries of the interaction Hamiltonian meant that any choice of the VLF or OBR criteria was equally useful, with all three giving comparable results.

However, we do find that with the present system the three-mode EPR correlations (C_{ij}^{OBR}), which are defined using the properties of one quadrature to infer properties of a combined quadrature that involves the other two modes, are operationally useful. As shown in Figs. 5 and 6, there is an
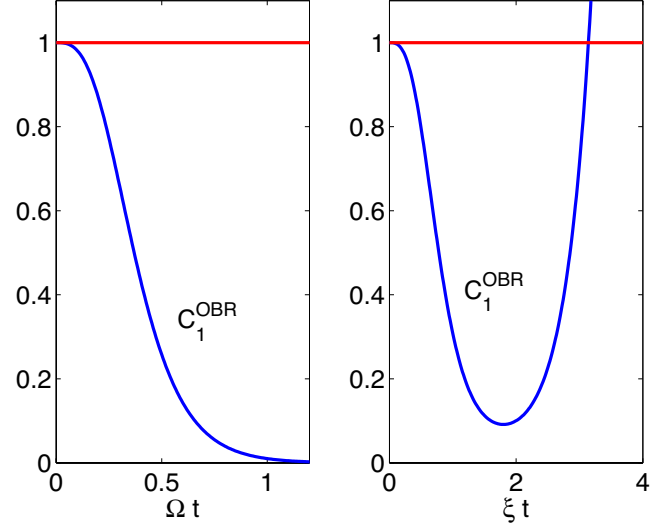

FIG. 4. (Color online) The analytical solutions of the OBR two-mode inference correlations. On the left-hand side, $\kappa_1 = 1.2\kappa_2$, while on the right-hand side $\kappa_2 = 1.8\kappa_1$. Although all three correlations should be below 1 to demonstrate genuine tripartite entanglement, in each case only one of them (C_1^{OBR}) goes below this level, while the other two are both exactly equal to 1.

unambiguous demonstration of the inseparability of the density matrix almost as soon as the interaction begins. This demonstration continues well past the point where the undepleted pump approximation is expected to lose its validity. Hence, if entanglement were to be demonstrated experimentally with this scheme, measurement of either these three correlations or else V_{123} would be the preferred options. Which is the best correlation to measure in a given situation can be seen in Fig. 7, where we have plotted the optimum performance of the criteria as a function of interaction strength. We see that, in general for this system, the preferred
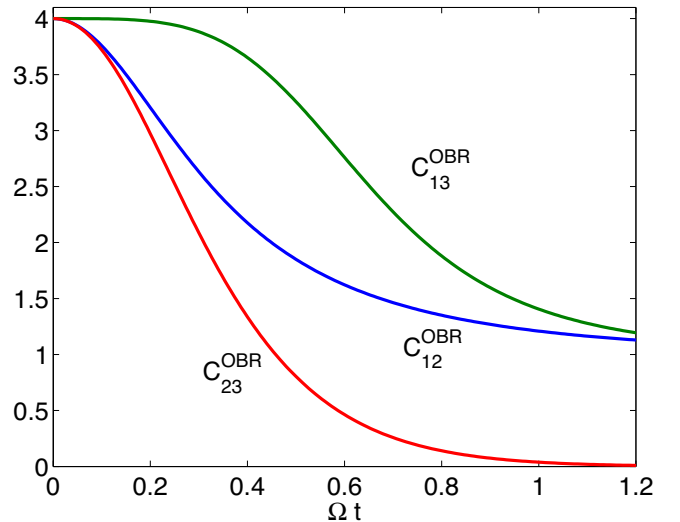

FIG. 5. (Color online) The analytical solutions of the OBR correlations which infer combined mode properties from those of a single mode, with $\kappa_1 = 1.2\kappa_2$. All three correlations should be below 4 to demonstrate genuine tripartite entanglement.
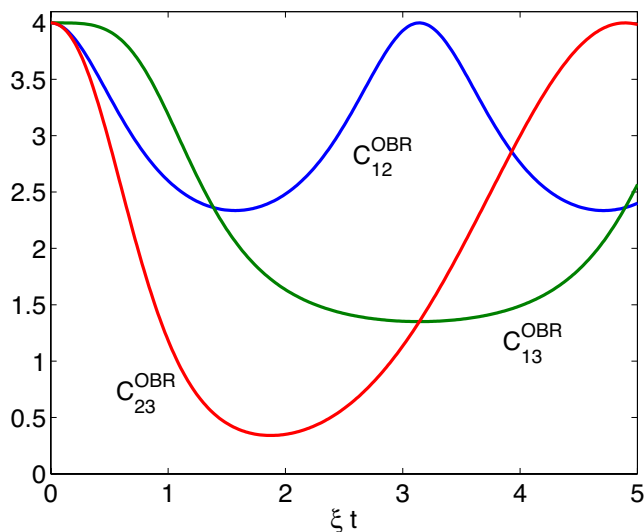
FIG. 6. (Color online) The analytical solutions of the OBR correlations which infer combined mode properties from those of a single mode, with $\kappa_2 = 1.8\kappa_1$. All three correlations should be below 4 to demonstrate genuine tripartite entanglement.

correlation to measure is V_{123}, although its success in this specific case does not indicate its superiority for all possible asymmetric schemes.

V. CONCLUSIONS

We have examined the interlinked $\chi^{(2)}$ interaction scheme of Bondani *et al.* [1] in terms of its suitability for producing output fields that exhibit genuine tripartite entanglement and shown that it can produce three fully entangled fields at different frequencies. We have calculated correlations using three different approaches, one that uses the properties of combined quadratures and may be optimized, and the other two that use three-mode generalizations of the EPR argument. We find that these correlations give different answers to the question of whether tripartite entanglement is present in a particular regime, with some giving false negatives. The fact that the correlations give different answers is not
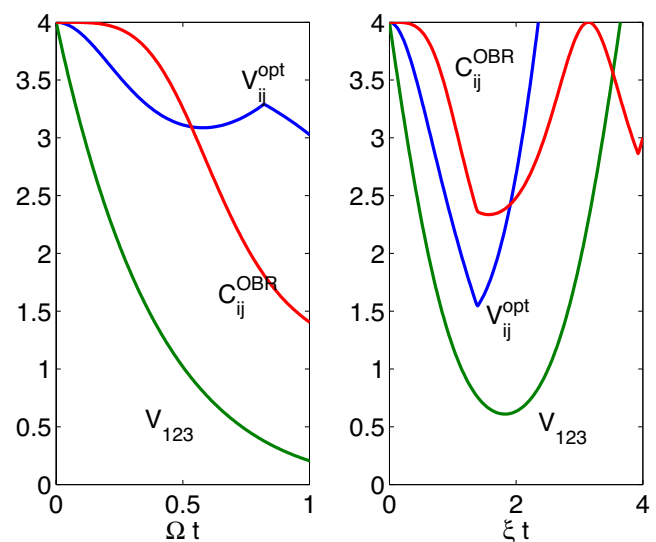

FIG. 7. (Color online) The best performance of the different criteria as functions of the interaction strength, for $\kappa_1 = 1.2\kappa_2$ (left) and $\kappa_2 = 1.8\kappa_1$ (right). For any of the correlations shown, a value of less than 4 signifies genuine tripartite entanglement. For V_{ij}^{opt} of Eq. (11), we take the second lowest value as two of the inequalities must be violated, while for C_{ij}^{OBR} we take the highest value as three inequalities must be violated.

contradictory as they all have been proven to provide sufficient but not necessary criteria, and this is a good example of how investigations of continuous-variable entanglement become more complicated once we have more than two modes involved. This is especially the case for asymmetric schemes, as the availability of merely sufficient but not necessary criteria means that it will not always be obvious *a priori* which correlations should be measured. Finally, we note that the unreliability of some of the correlations is not an operational problem, as all the criteria we have used here can be investigated using the same set of operator moments.

[1] M. Bondani, A. Allevi, E. Gevinti, A. Agliati, and A. Andreoni, Opt. Express **14**, 9838 (2006).

[2] J. Jing, J. Zhang, Y. Yan, F. Zhao, C. Xie, and K. Peng, Phys. Rev. Lett. **90**, 167903 (2003).

[3] T. Aoki, N. Takei, H. Yonezawa, K. Wakui, T. Hiraoka, A. Furusawa, and P. van Loock, Phys. Rev. Lett. **91**, 080404 (2003).

[4] J. Guo, H. Zou, Z. Zhai, J. Zhang, and J. Gao, Phys. Rev. A **71**, 034305 (2005).

[5] A. Ferraro, M. G. A. Paris, M. Bondani, A. Allevi, E. Puddu, and A. Andreoni, J. Opt. Soc. Am. B **21**, 1241 (2004).

[6] A. S. Bradley, M. K. Olsen, O. Pfister, and R. C. Pooser, Phys. Rev. A **72**, 053805 (2005).

[7] M. K. Olsen and A. S. Bradley, J. Phys. B **39**, 127 (2006).

[8] N. B. Grosse, W. P. Bowen, K. McKenzie, and P. K. Lam, Phys. Rev. Lett. **96**, 063601 (2006).

[9] G. Giedke, B. Kraus, M. Lewenstein, and J. I. Cirac, Phys. Rev. A **64**, 052303 (2001).

[10] P. van Loock and A. Furusawa, Phys. Rev. A **67**, 052315 (2003).

[11] M. K. Olsen, A. S. Bradley, and M. D. Reid, J. Phys. B **39**, 2515 (2006).

[12] A. Einstein, B. Podolsky, and N. Rosen, Phys. Rev. **47**, 777 (1935).

[13] E. Schrödinger, Naturwiss. **23**, 807 (1935).

[14] M. D. Reid, Phys. Rev. A **40**, 913 (1989).

[15] M. D. Reid and P. D. Drummond, Phys. Rev. A **40**, 4493 (1989).

[16] M. D. Reid, in *Quantum Squeezing*, edited by P. D. Drummond and Z. Ficek (Springer, Berlin, 2004).

[17] S. M. Tan, Phys. Rev. A **60**, 2752 (1999).

[18] Z. Y. Ou, S. F. Pereira, H. J. Kimble, and K. C. Peng, Phys. Rev. Lett. **68**, 3663 (1992).

[19] L.-M. Duan, G. Giedke, J. I. Cirac, and P. Zoller, Phys. Rev. Lett. **84**, 2722 (2000).

[20] R. Simon, Phys. Rev. Lett. **84**, 2726 (2000).

[21] G. Adesso, A. Serafini, and F. Illuminati, e-print quant-ph/0609071.

[22] M. E. Smithers and E. Y. C. Lu, Phys. Rev. A **10**, 1874 (1974).

[23] M. G. Raymer, P. D. Drummond, and S. Carter, Opt. Lett. **16**, 1189 (1991).

[24] P. Kinsler, M. Fernée, and P. D. Drummond, Phys. Rev. A **48**, 3310 (1993).